China Instrument and Control Society
Instrumentation
INSTRUMENTATION, Vol. 13, No. 1, March 2026
https://doi.org/10.15878/j.instr.202600326

Article-Intelligent Detection & Fault Diagnosis

Advancing Automated Liquid-Handling Systems: Development and Evaluation of a Nonlinear Error-Compensated Air-Displacement Pipettor

Jun Lu[1,2*†], Zhizhong Zhang[1†], Qingqing Ye[1], Sheng Zhang[1], Jianqiang Chen[1], Yuanhua Wang[1], Guodong Sun[3], Zhiyong Sun[1], Jisheng Qin[1], Jianhua Dong[1], Shiwen Mai[1], Fengxiang Zhang[1], Xiaohui Wen[1], Xiao Zhang[1*], Guanglei Zhao[2*], Xueping Chen[1*]

[1] Guangzhou Institutes of Biomedicine and Health, Chinese Academy of Sciences, Guangzhou 510530, People's Republic of China

[2] School of Light Industry and Engineering, South China University of Technology, Guangzhou 510641, People's Republic of China

[3] Guangzhou Koalson Smart Manufacturing Technology Co., Ltd.,Guangzhou 510000, People's Republic of China

[*] Corresponding author email: zhang_xiao@gibh.ac.cn (X. Z.), chen_xueping@gibh.ac.cn (X. C.), glzhao@scut.edu.cn(G. Z.), lu_jun@gibh.ac.cn (J. L.)

[†] These authors contributed equally to this work

Abstract: This study introduces a nonlinear error-compensated air-displacement pipettor (NEC_ADP), a novel system that addresses the key limitations in commercial pipetting setups. By incorporating nonlinear error-compensation (NEC) technology, the NEC_ADP improves the accuracy and precision of liquid handling across a wide range of volumes, from micro-volumes (1 μL) to macro-volumes (up to 1000 μL), and for reagents with varying viscosities and surface tensions. Unlike conventional pipettors, which rely on linear compensation or manual recalibration, NEC_ADP features real-time, online calibration, eliminating the need for factory recalibration and reducing maintenance costs. The system was built with a modular design, allowing seamless scalability from single- to multi-channel configurations. It integrates effortlessly with existing laboratory systems using the open platform communications unified architecture (OPC UA), enhancing interoperability and automation. In addition, the use of machine-learning algorithms for motion control and trajectory planning ensures optimal pipetting strategies and automatic adaptation to different reagents and volumes. This study demonstrates the superior performance of NEC_ADP compared to commercial systems, including the TECAN Cavro® and Eppendorf epMotion®, with significant improvements in accuracy and precision. Innovation in NEC_ADP technology and system integration marks a significant advancement in automated liquid handling, offering robust support for high-precision applications in fields such as genomics, stem-cell research, and synthetic biology.

Keywords: nonlinear error compensated air displacement pipettor (NEC_ADP); open platform communications unified architecture (OPC UA); automated liquid handling; curve regression and motion control; online accuracy calibration

Citation: Jun Lu, Zhizhong Zhang, Qingqing Ye, Sheng Zhang, Jianqiang Chen, Yuanhua Wang, Guodong Sun, Zhiyong Sun, Jisheng Qin, Jianhua Dong, Shiwen Mai, Fengxiang Zhang, Xiaohui Wen, Xiao Zhang, Guanglei Zhao, Xueping Chen."Advancing Automated Liquid-Handling Systems: Development and Evaluation of a Nonlinear Error-Compensated Air-Displacement Pipettor." Instrumentation 13, no. 1 (March 2026). https://doi.org/10.15878/j.instr.202600326

1 Introduction

Pipettors are commonly used laboratory tools for liquid transfer and handling. Liquid handling is a fundamental process in biology, chemistry, and medicine. It plays a critical role in drug development, bioprocess-based manufacturing, and fundamental research, such as high-throughput screening, assay preparation in genomics and proteomics, and clinical diagnostics[1]. Manually handled pipettors rely on air pressure or piston movement (pressing and releasing the piston are used to control the aspiration and liquid dispensing). Manual pipettors are sufficiently flexible for small-scale experiments, but precision requires skilled operation[2].

Motor-driven air-displacement pipettes (ADPs) integrate pipetting modules, control modules, and software, automating liquid handling and significantly improving efficiency and accuracy. ADPs are suitable for high-throughput, large-scale biopharmaceutical production and genetic-sequencing experiments[3]. They minimise human error, enhance experimental reliability and reproducibility, and can be integrated with other devices to promote automation and intelligent laboratory workflows. ADPs play a critical role in automated laboratories owing to their high precision, reproducibility, and versatility, making them indispensable in research and production. Many well-known manufacturers worldwide are currently engaged in the research and development of automated ADPs, as shown in Table 1.

However, as outlined in Table 1, commercial ADP systems such as the Hamilton Microlab® VANTAGE[4-7], TECAN Cavro® Series[8-13], and Eppendorf epMotion®[14-20] exhibit key operational limitations in real-world laboratory settings. The ADP application in laboratories have accuracy deviations, limited operational-efficiency, and are difficult to integrate with laboratory systems as discussed below.

a. Accuracy and precision limitations: Commercial ADP systems often exhibit performance degradation due to factors such as component wear, liquid property variations, and environmental changes. Table 1 contrasts their nominal specifications with real-world challenges, justifying the need for nonlinear compensation.

b. High maintenance and calibration costs: As highlighted in the table, most ADPs require high maintenance costs and inconvenient upkeep, often necessitating factory recalibration, which hampers operational efficiency.

c. Complex system integration: System integration is complex due to the varying control protocols and interface standards across manufacturers, which makes integrating ADP with other laboratory systems difficult. Current ADP systems rely on vendor-specific protocols, complicating multi-brand automation. Our OPC UA-based framework enables plug-and-play interoperability (e. g., Danaher Group collaboration), which can reduce the integration time.

Solutions and improvements in pipetting technology are required for widespread ADP adoption and optimisation.

High-precision ADP control systems require stability and accuracy. Deviations in movement—whether excessive or insufficient—can compromise accuracy; effective regulation of acceleration and speed requires advanced trajectory planning and interpolation algorithms for optimising the pipetting path and minimising potential errors[21]. Minimising friction and vibration among mechanical components using lubricants and vibration-damping measures further supports smooth system operation. Regular maintenance and calibration are vital for sustaining peak performance and measurement precision.

Acceleration, speed control, and precise trajectory planning are the key elements for achieving pipetting accuracy. Widely adopted motion-control algorithms include the trapezoidal profile, S-curve profile[22], cubic-spline interpolation, and dog-legged motion[23]. The trapezoidal profile produces stable linear movements, whereas the S-curve profile minimises oscillations by smoothing the acceleration, thus enhancing movement stability. Cubic-spline interpolation generates continuously differentiable curves suitable for complex trajectory planning, and the dog-legged motion algorithm optimises path planning under constraints. By integrating the S-curve and cubic-spline interpolation algorithms within ADP systems, it is possible to achieve high-precision, low-vibration movement, thus enhancing the pipetting accuracy and operational efficiency.

ADP requires regular maintenance and calibration for ensuring both accuracy and precision in liquid handling. Standard calibration techniques include gravimetric, colourimetric, volumetric, and comparative methods[24,25]. Gravimetric calibration involves weighing a specific volume of liquid and comparing it to the pipettor reading to verify the accuracy. Colourimetric calibration uses a solution of known concentration, and the optical density of the dispensed liquid is measured and compared to that of the original solution using spectrophotometers or colourimetric reagents. Volumetric calibration assesses the accuracy of a pipettor by dispensing it into a calibrated container and comparing the initial and post-dispensing liquid levels. Gravimetric calibration weighs a precisely measured solution and records the weight changes after dispensing. Comparative calibration involves using a previously calibrated pipettor to assess the test-pipettor volume by dispensing liquids side by side.

These calibration methods are essential for identifying and correcting deviations and ensuring reliable and accurate liquid transfer in practical applications. However, many current ADPs require factory-based recalibration, limiting field operations, and increasing maintenance complexity and costs[26]. Therefore, there is a growing demand for calibration

Table 1 Performance comparison of well-known, automated, Air Displacement Pipettors (ADPs) worldwide

	Single-channel			Eight-channel	96-channel
Air Displacement Pipettor	 Hamilton ZEUS	 Eppendorf epMotion®	 Tecan Cavro®	 Eppendorf epMotion®	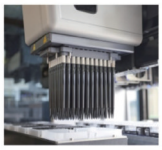 Hamilton CO-RE 96
Volume range	1 - 1000 µL	0.2-1000uL	1 - 1000 µL	1 - 1000 µL	1 - 1000 µL
Multiple device spacing	18mm	No	18mm	No	—
Accuracy	<1% at 1000 µL, <5% at 1 µL	<0.7% at 1000 µL(TS1000), <5% at 1 µL(TS10)	<1% at 1000 µL, <5% at 1 µL	<0.8% at 1000 µL(TS1000), <7.5% at 1 µL	<1% at 1000 µL, <5% at 1 µL
Precision	<0.75% at 1000 µL, <4% at 1 µL	<0.15% at 1000 µL(TS1000), <3% at 1 µL(TS 10)	<0.75% at 1000 µL, <6% at 1 µL	<0.15% at 1000 µL(TS1000), <5% at 1 µL(TS10)	<1% at 1000 µL, <5% at 1 µL
Product Series	ZEUS X1 ZEUS 5mL ZEUS LT	TS 10(0.2-10µL) TS 50(1-50µL) TS 300(20-300µL) TS 1000(40-1000µL)	Cavro ®	TS 10-8 TS 50-8 TS 300-8 TS 1000-8	CO-RE 96 Probe Head
Calibration and maintenance	Factory calibration,return to Factory for Maintenance	200,000 runs for inspection, with at least 1 calibration annually	Factory calibration, Maintenance-free design	200,000 runs for inspection, with at least 1 calibration annually	Factory calibration,return to Factory for Maintenance
Communication	RS-232 or CAN (Hamilton Protocol)	epMotion Protocol	RS-485 , CAN	epMotion Protocol	Only applied in the Microlab STAR Line
Tip compatibility	10µl, 50µl, 300µl, 1000µl tips	10µl, 50µl, 300µl, 1000µl tips	10µl, 50µl, 300µl, 1000µl tips	10µl, 50µl, 300µl, 1000µl tips	10µl, 50µl, 300µl, 1000µl tips
Nonlinear Error Compensated	No	No	No	No	No
Online Calibration	No	No	No	No	No
Automated Integration	Yes	Compatible only with epMotion software epBlueTm	Yes	The epMotion series platforms for diverse automated liquid handling	applied in the Microlab STAR Line

methods that allow rapid onsite adjustments, reducing the need for factory returns, streamlining maintenance, and cost efficiency.

Various approaches exist for integrating modular systems into laboratory automation, including interface integration, middleware integration, custom scripting, radio-frequency identification (RFID)/barcode integration, and automated script integration. Interface integration employs standard communication protocols, such as the hypertext transfer protocol, representational state transfer, and simple object access protocol, often utilising application programming interfaces (APIs) or software development kits provided by manufacturers to connect pipetting systems with laboratory information

management systems (LIMS). Middleware integration uses software platforms such as LabVIEW to facilitate data exchange and improve data-management efficiency. Customised scripts, frequently developed in languages such as Python or C++, enable tailored data transfer and command execution through an in-depth knowledge of the system APIs. RFID/barcode integration uses automatic identification technologies to link pipettors with specific samples, enabling automatic data capture and seamless transmission to LIMS.

However, the lack of standardised interfaces across the current ADP market presents significant challenges to automation integration. Automation processes have become increasingly complex and resource-intensive, with each manufacturer adopting distinct communication protocols. The adoption of standardised protocols is critical to solve this problem. Standardised protocols streamline laboratory operations, enabling seamless device integration across different manufacturers, while ensuring data traceability and reliability, which are key factors that support robust scientific decision-making. A unified platform for integration also enables efficient experimental design, comprehensive data analysis, and optimised report generation, further advancing laboratory automation and enhancing intelligent workflow capabilities[27-29].

We developed an innovative automated nonlinear error-compensation air-displacement pipettor (NEC_ADP), distinguished by its application in nonlinear error-compensation (NEC) technology. The decision tree[30] acts as an auxiliary tool to dynamically optimize parameters for this core innovation technology. Our pipettor constructs a precise error-compensation model by accurately measuring the complex, nonlinear relationship between the motor displacement and pipetted volume. This model dynamically adjusts the motor-control commands in real time, significantly enhancing pipetting accuracy. Moreover, we developed a specialised database for pipetting experiments across a variety of reagents with different properties. The reagents used were deionised water, ethanol (polar, with relatively few hydrogen bonds, and volatile), glycerol (high viscosity), and phosphate-buffered saline (PBS). We leveraged decision-tree algorithms from machine learning to enable intelligent and automatic matching of motion-control and trajectory-planning strategies for these reagents. This approach ensures that NEC_ADP maintains pipetting precision and accuracy across different reagents, providing robust support for biological research, pharmaceutical development, and clinical-diagnostic applications(Fig. 1).

The NEC_ADP has broad applications in life-science equipment. These include, but are not limited to, fully automated, large-scale, mesenchymal-stem-cell preparation systems, high-throughput and high-sensitivity diagnostic-automation platforms, synthetic biology-research automation systems, and equipment for constructing high-depth genomic libraries.

2 Materials and Methods

2.1 Mechanical Design of NEC_ADP

The core components of the NEC_ADP system include a liquid-aspiration mechanism, tip-ejection system, tip-attachment system, auxiliary positioning, and control system, which enable reliable pipetting performance across various well-plate specifications. The manufacturers and models of the key core components used in this study are consistent with those described in our previous work[31].

2.1.1 Liquid-Aspiration Mechanism

This system converts the rotational motion of the motor into linear motion (using a lead-screw transmission), driving a plunger along a guide rod to vary the working volume inside the pipette tip - to enable liquid aspiration and dispensing. The system was designed for easy disassembly to facilitate the regular replacement of sealing components, as sealing is crucial to ensuring long-term precision.

2.1.2 Tip-Ejection System

Tip ejection is achieved by the downward movement of the plunger rod, which makes contact with the ejection-rod handle and pushes the rod down to release the pipette tip. Upon resetting, the ejection rod automatically returns to its original position.

2.1.3 Tip-Attachment System

A pneumatic actuator drives the tip-attachment mechanism along a guide rail and slides rapidly to ensure secure and stable fitting between the pipette tip and nozzle through inertia.

2.1.4. Auxiliary Positioning and Control System

This system monitors the tip loading using sensors equipped for robust calibration and ensures accurate zero-point reference positioning. It provides timely feedback in the event of malfunction to aid maintenance.

The system was configured into various multichannel modes to satisfy different pipetting requirements - based on the design principles of the single-channel air-displacement pipettor NEC_ADP1_1. The multichannel modes included the four-channel-independent and arrayed NEC_ADP1_4 configurations, and the eight-channel-independent and arrayed NEC_ADP1_8 NEC_ADP4_8 configurations (Fig. S4). These designs are adaptable to a wide range of applications, providing precise pipetting, dispensing, liquid handling, and mixing functions, while being compatible with multiple-well plate formats.

The design features a compact structure and a comb-like modular configuration, allowing flexible adaptation to 24-well, 96-well, and 384-well plates. It can be easily

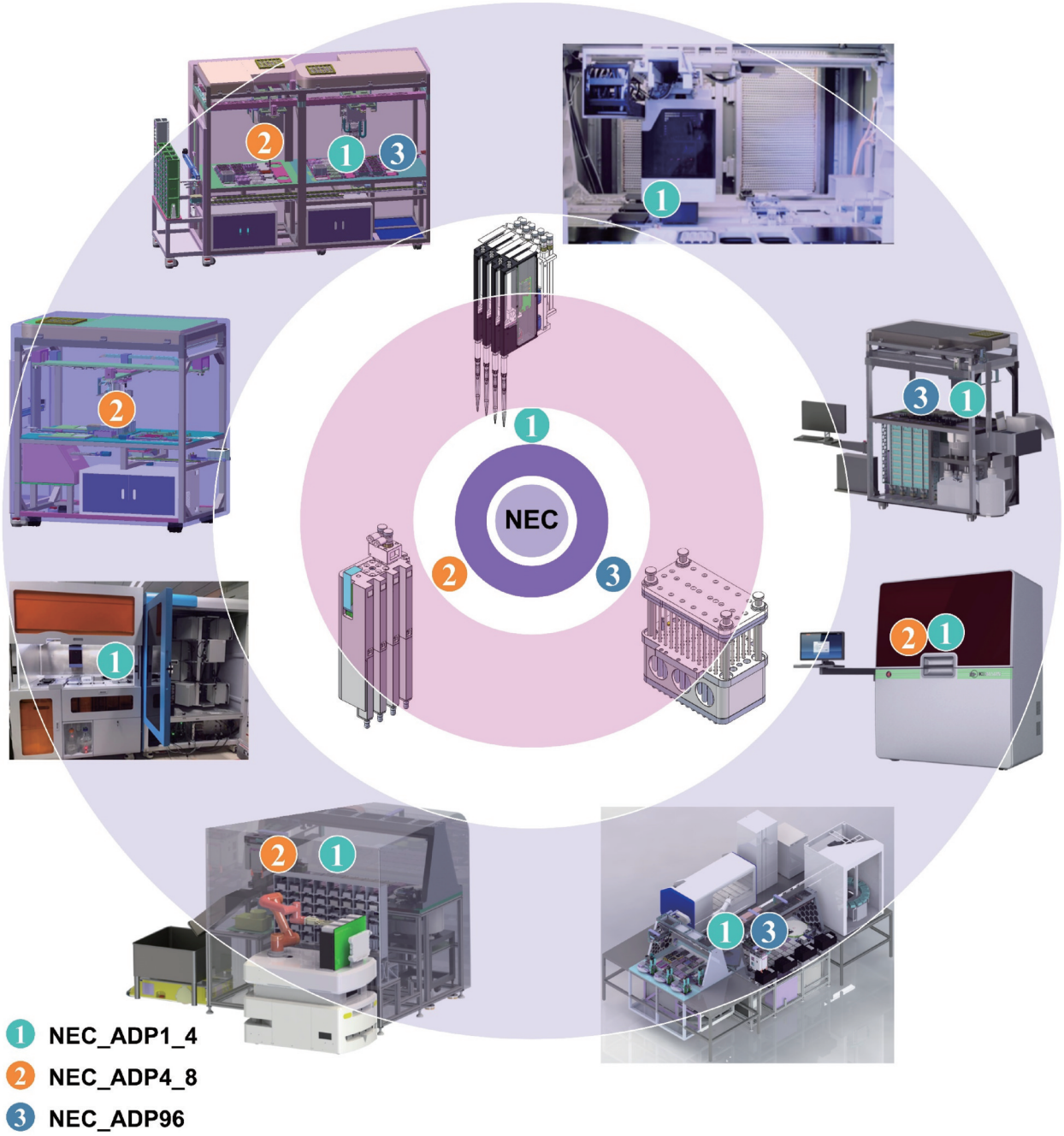

Fig.1 Three Typical Configurations and Applications of the Air-Displacement Pipettor (NEC_ADP) Based on Nonlinear Error-Compensation (NEC) Technology. ①*Single-Channel Pipette NEC_ADP_1*: The NEC_ADP_1 can be expanded from a single channel to an 8-channel configuration (NEC_ADP1_1 to NEC_ADP1_8) using an equidistant arrangement. In the figure, NEC_ADP1_4 represents the four-channel version. NEC_ADP_1 is primarily used for flexible single or synchronized pipetting operations. ②*Inline Pipette NEC_ADP_4*: The NEC_ADP_4 features 4-channel pipetting capability and can be used in an interleaved configuration to create an 8-channel setup (NEC_ADP4_8) by pairing two NEC_ADP_4 units. This design is optimized for parallel pipetting in a single row. ③*96-Channel Integrated Pipette NEC_ADP_96*: The NEC_ADP_96 is specifically designed for 96-channel multi-row parallel pipetting tasks, making it ideal for high-throughput applications.

reconfigured to accommodate the NEC_ADP1_1, NEC_ADP1_4, and the eight-channel NEC_ADP1_8 modes. Building on the design concept of the four-channel arrayed NEC_ADP_4, we developed a 96-channel integrated pipettor, NEC_ADP_96, that supports high-throughput applications in 96-well plate formats (Fig. S4), which caters to a wide range of pipetting scenarios.

2.2 NEC_ADP Accuracy Measurements

To evaluate the accuracy of the NEC_ADPs, we used a gravimetric method as the core measurement technique[24,25]. The experimental conditions were strictly controlled, and the room temperature was maintained at 20 ± 5 ℃ to ensure the stability and reliability of the results. Distilled water was used as the testing medium, with its temperature kept within 2 ℃ of the room

temperature to minimise any potential effects of temperature fluctuations on the results.

The experimental procedure follows. A high-precision balance (BT25S, Sartorius, Germany; maximum capacity = 21 g, resolution = 0.01 mg) was securely positioned on the workstation. A weighing cup was placed at the centre of the balance, and after the reading was stabilised, precise zero calibration was performed to ensure measurement accuracy. The pipettor module was mounted vertically on a specialised stand on the workstation and operated as an independent unit (without being integrated into its final system). The module was connected to a PC using a serial cable, allowing remote control and data recording (Fig. S1A).

During the preparation phase, distilled water was poured into the designated liquid reservoir to obtain a stable liquid surface. The pipette tips were placed neatly on a tip rack for automatic loading. The pipettor module automatically performed tip loading and initialisation through a preset program, including three aspiration/dispense cycles, to thoroughly wet the inner surface of the tip, thereby reducing the risk of liquid retention, which could affect accuracy.

During testing, a pre-programmed script on a PC precisely controlled the actions of the pipetting module. The pipette tip was then slowly immersed in distilled water to a depth of 5 mm below the surface. The module then aspirated a preset volume of water. After aspiration, the tip was raised and moved above the weighing cup, where water was dispensed. This process was repeated multiple times and balance readings were recorded after each cycle. The average value of multiple measurements was used to determine the actual weight of the distilled water.

The actual volume of water was calculated using the actual water weight and the known density. This value was compared with the set volume of the pipettor, and the absolute difference between the two was considered the error. Finally, the set volume was divided by the error to calculate the pipetting accuracy. This metric reflects the performance of the NEC_ADP, as shown in Fig. S1.

The information on experimental procedures for other solvents is the same as for water.

2.3 NEC Model of the NEC_ADP

The working principle of a piston-driven pipettor is based on the relationship between air pressure and volume changes, as described by Boyle's law [32]. In an ideal gas, the pressure and volume are inversely proportional and the relationship is expressed by $PV = nRT$, where P is the pressure, V is the volume, n is the amount of gas, R is the gas constant, and T is the temperature. However, in practice, the compression of air is influenced by real gas behaviour, leading to a nonlinear relationship between pressure and volume. To address this problem, a nonlinear error-compensation model must be developed to correct pipetting errors.

For ease of analysis, we introduce a parameter called *Resolution_SV* (pipetting resolution, in steps/μL), which represents the relationship between the smallest motor step and the pipetted volume. For example, consider the motor to have 4096 steps per revolution, the piston movement to be 1 mm, and the piston diameter to be 5 mm.

$$Pipetting\ Volume = \pi r^2 = \pi(2.5^2) = 6.25\pi\ \mu L$$

Thus, the motor step value for 1 μL would be:

$$Resolution\_SV = 4096/(6.25\pi) = 208.607\ (step)$$

Note: In an ideal-gas compression scenario, *Resolution_SV* would remain constant at 208.607 *steps/μL*.

However, in real-world applications, because of the nonlinear compression of air, *Resolution_SV* becomes variable. By developing a curve equation for *Resolution_SV* at different target pipetting volumes, we can compensate for the pipetting errors. Because theoretical modelling is complex owing to the many factors affecting air compression, we chose to use experimental measurements. By collecting *Resolution_SV* data at multiple points and generating regression curves, we were able to calculate the appropriate motor steps for a given pipetting volume.

Below, we use the single-channel NEC_ADP1_1 as an example to demonstrate the measurement of *Resolution_SV* using a method similar to that used for pipetting accuracy, employing the gravimetric method.

2.3.1 Measurement of Resolution_SV for 1000-μL Pipette Tip and Generating a Regression Curve

Through multiple experiments, we obtained data for the actual pipetting volume and the corresponding *Resolution_SV* values (Table S6). For a 1000 μL tip, the motor step value for 1 μL of liquid is shown in Fig. S3B) with the regression curve-based *Resolution_SV* (Fig. S3C) below.

$$y = -0.0048x^2 + 219.98x + 267.98\ (R^2 = 0.999999)$$

where x is the target *volume*, and y is the motor-command position.

2.3.2 Measurement of Resolution_SV for a 50-μL Tip and Regression-Curve Generation

Similarly, for a 50- μL tip, we conducted multiple experiments to obtain seven data points for actual pipetting volume and *Resolution_SV* values (Table S6). The regression curves are shown in Fig. S3B using the following equation:

$$y = 0.1139x^2 + 210.6x + 192.65\ (R^2 = 0.999956)$$

where x is the target volume, and y is the motor-command position.

2.3.3 Calculating the Motor-Command Position with Compensation

When the system receives a pipetting command, the target pipetting volume is substituted into the regression equation to calculate the motor step position. For

instance, if the target pipetting volume is 300 μL, substitution into the Regression Equation (1) results in the following.

$$y = -0.0048 \times 300^2 + 219.98 \times 300 + 267.98 = 65830\ (steps)$$

Therefore, the corrected Resolution_*SV* is:

$$Resolution\_SV = 65830/300 = 219.4\overline{3}\ (steps/\mu L)$$

Similarly, for a target pipetting volume of 30 μL, using Regression Equation (2):

$$y = 0.1139 \times 30^2 + 210.6 \times 30 + 192.65 = 6613\ (steps)$$

Therefore, the corrected Resolution_SV is:

$$Resolution\_SV = 6613/30 = 220.43\overline{3}\ (steps/\mu L)$$

2.3.4 NEC_ADP Motion-Control Planning

The core principle of an ADP is the precise movement of the piston-driving motor, for accurate liquid transfer. After calculating the compensated motor step for the target pipetting volume, the next challenge was to implement an accurate motor-motion control. The pipetting control process comprised the following steps:

A. *Receiving the Pipetting Command*

NEC_ADP receives a command that typically includes parameters such as pipetting speed, acceleration, and target volume.

B. *Pipetting Speed-Curve Planning*

The pipetting speed curve is determined based on pipetting parameters, which generally include acceleration, constant velocity, and deceleration phases. The pipetting speed curve describes the change in the speed over time (Fig. S5A). The speed can be expressed as

$$\begin{cases} v(t) = -\dfrac{4A_{mp}}{3T_1^2}t^3 + \dfrac{2A_{mp}}{3T_1}t^2 + V_s & t \in [T_0, T_1] \\ v(t) = V_M & t \in (T_1, T_2] \\ v(t) = \dfrac{4A_{mm}}{3(T_3 - T_2)^2}(t - T_2)^3 - \dfrac{2A_{mm}}{3(T_3 - T_2)} & (t - T_2)^2 + V_M \quad t \in (T_2, T_3] \end{cases} \tag{1}$$

The pipetting process can be divided into three phases: acceleration *[T_0, T_1]*, constant velocity *(T_1, T_2]*, and deceleration *(T_2, T_3]*.

v(t) denotes the instantaneous pipetting velocity of the device at any given time *t*.

The pipetting process typically has an initial velocity V_S of zero.

V_M is the predetermined target speed for the pipetting operation as specified in the pipetting instructions.

A_{mp} represents the acceleration rate programmed into the pipetting instructions; it controls the rate of speed increase during the acceleration phase.

A_{mm} is the programmed deceleration rate; it governs the rate of decrease in speed during the deceleration phase.

T_1 indicates the moment when, owing to the acceleration A_{mp}, the pipetting speed reaches its target speed V_m.

T_3 indicates the moment when, owing to the deceleration A_{mm}, the pipetting speed decelerates back to zero.

The total duration of the pipetting operation, from start time T_0 to end time T_3, constitutes the overall pipetting time.

C. *Time Calculation for Acceleration and Deceleration Phases*

By substituting $t = T_1$ into Equation (1), the following equation is obtained.

$$V_M = -\frac{4A_{mp}}{3T_1^2}T_1^3 + \frac{2A_{mp}}{3T_1}T_1^2 + V_s \tag{2}$$

Therefore, the time T_1 required to accelerate from V_S to V_M is obtained.

$$T_1 = \frac{3(V_M - T_S)}{2A_{mp}} \tag{3}$$

By substituting $t = T_3$ into Equation (1), the duration of the deceleration phase *(T_3 - T_2)* is obtained.

$$T_3 - T_2 = \frac{3(V_M - T_E)}{2A_{mm}} \tag{4}$$

D. Pipetting-Volume Calculation

Integrating Equation (2) yields the curve of the dispensing displacement as it varies with time (Fig. S5A); it is represented by the following Equation (5).

$$\begin{cases} s(t) = -\dfrac{A_{mp}}{3T_1^2}t^4 + \dfrac{2A_{mp}}{3T_1}t^3 + V_s{*}t & t \in [T_0, T_1] \\ s(t) = V_M(t - T_1) + S_1 & t \in (T_1, T_2] \\ s(t) = \dfrac{4A_{mm}}{3(T_3 - T_2)^2}(t - T_2)^4 - \dfrac{2A_{mm}}{3(T_3 - T_2)}(t - T_2)^3 + V_M(t - T_2) + S_2 & t \in (T_2, T_3] \end{cases} \tag{5}$$

Note: Equation (5) represents the corresponding motor-movement displacement *s(t)* at time *t*.

When $t = T_1$, substituting it into Equation (5) yields the dispensing displacement during the acceleration phase.

$$S_1 = \frac{3}{4}\frac{\left(V_M^2 - V_S^2\right)}{A_{mp}} \tag{6}$$

Similarly, the dispensing displacement during the deceleration phase can be obtained.

$$S_3 = \frac{3}{4}\frac{\left(V_M^2 - V_E^2\right)}{A_{mm}} \tag{7}$$

Based on the target dispensing volume, S_0, the motor displacement during the constant-velocity phase is

derived as shown in Equation (8).

$$S_2 - S_1 = S_0 - S_1 - S_3 = S_0 - \frac{3}{4}\frac{\left(V_M^2 - V_S^2\right)}{A_{mp}} - \frac{3}{4}\frac{\left(V_M^2 - V_E^2\right)}{A_{mm}} \tag{8}$$

2.3.5 Constant-Velocity Time Calculation

Constant-velocity time is T_2-T_1 which is substituted into Equation (8).

$$T_2 - T_1 = \frac{S_2 - S_1}{V_M} = \frac{S_0}{V_M} - \frac{3}{4V_M}\left(\frac{\left(V_M^2 - V_S^2\right)}{A_{mp}} + \frac{\left(V_M^2 - V_E^2\right)}{A_{mm}}\right) \tag{9}$$

T_2 is given by Equation (10).

$$T_2 = \frac{S_0}{V_M} - \frac{3}{4V_M}\left(\frac{\left(V_M^2 - V_S^2\right)}{A_{mp}} + \frac{\left(V_M^2 - V_E^2\right)}{A_{mm}}\right) + T_1 = \frac{S_0}{V_M} - \frac{3}{4V_M}\left(\frac{\left(V_M^2 - V_S^2\right)}{A_{mp}} + \frac{\left(V_M^2 - V_E^2\right)}{A_{mm}}\right) + \frac{3\left(V_M - T_S\right)}{2A_{mp}} \tag{10}$$

T_3 is given by Equation (11).

$$T_3 = T_2 + \frac{3\left(V_M - T_E\right)}{2A_{mm}} = \frac{S_0}{V_M} - \frac{3}{4V_M}\left(\frac{\left(V_M^2 - V_S^2\right)}{A_{mp}} + \frac{\left(V_M^2 - V_E^2\right)}{A_{mm}}\right) + \frac{3\left(V_M - T_S\right)}{2A_{mp}} + \frac{3\left(V_M - T_E\right)}{2A_{mm}} \tag{11}$$

Note: T_1 represents the duration of the acceleration phase, T_2-T_1 represents the duration of the constant-velocity phase, T_3-T_2 represents the duration of the deceleration phase, and T_3 represents the total dispensing phases, respectively.

The NEC_ADP system could plan and execute precise motor control to ensure accurate and efficient liquid transfer by following the above steps.

E. Motor-Interpolation Output

Using the interpolation cycle as the time reference and substituting Equations (1) and (5) into the calculation, we could accurately determine the changes in the motor speed and displacement during each interpolation cycle, as illustrated in Fig. S5B. These calculated speed and displacement commands were then precisely transmitted to the motor drive system, enabling NEC_ADP to achieve a highly accurate and smooth liquid transfer during operation.

Note: For an example of motion control planning, refer to the attached.

F. NEC_ADP Online Accuracy Calibration

Over time, the pipetting accuracy of NEC_ADP systems could decline owing to component wear and material aging, negatively impacting the reliability and precision of the experimental results. Therefore, the regular calibration of the pipetting control system is essential. As traditional calibration requires disassembling the pipettor and sending it back for professional maintenance (which is time consuming and expensive) we developed an innovative, fast, convenient, and cost-effective online-calibration method for pipettors. The online calibration process is outlined below.

I. Weighing-Based Online Standard-Liquid Transfer

This step mirrors the offline accuracy measurement process but integrates operations into the working environment. NEC_ADP remained integrated into the pipetting workstation, with the balance placed directly on the workstation surface. All previous manual actions, such as pipettor movement, aspiration, and dispensing, were fully automated using predefined scripts. These scripts also handled tasks such as tip priming (e. g. performing three aspiration and blowout cycles for new tips) and precisely controlling the robotic arm to position the tip above the distilled water and regulate the immersion depth and aspiration volume. After liquid aspiration, the robotic arm moved its tip to a weighing cup for precise dispensing.

II. Accuracy Calculation and Evaluation

The accuracy of the pipetting device was calculated by comparing the target pipetting volume with the actual volume (determined using a weighing method). The absolute value of the difference was used to determine the pipetting accuracy. This value was then compared with the preset accuracy thresholds to assess whether NEC_ADP required further calibration.

III. Resolution_SV Calibration

If the pipetting accuracy did not meet the required standards, calibration was initiated. Depending on the pipetting speed and volume, an appropriate calibration script was selected to fine-tune the pipetting device. Adjusting the Resolution_SV parameter directly affects the volume aspirated or dispensed per cycle, thereby improving the precision. To ensure comprehensive calibration, at least four different pipetting volumes were calibrated, and their respective Resolution_SV values were recorded.

IV. Regression Curve for Pipetting Volume and Motor Command

Based on multiple calibration data points of target pipetting volumes and their corresponding *Resolution_SV* values (Table S6, S8, S10), statistical analysis was used to generate regression curves that related pipetting volume to motor commands (Fig. 3B, Fig. 4C, Fig. 4E, Fig. 4G, Fig. 5C). The parameters of these regression curves were stored within the system for real-time use in future operations and error compensation.

G. Machine Learning and Decision Tree

A database (Table S2) was established to capture parameters such as density, viscosity, and surface tension for various reagents with distinct properties, including pure water, ethanol, glycerol, and PBS. Using a decision-tree algorithm, intelligent automated matching was achieved for motion-control and trajectory-planning strategies, including the leading air gap, aspirate, trailing

air gap, dispense motion speed (V_m), acceleration (A_{mp}), deceleration (A_{mm}), and volumes of the leading and trailing air gaps. The decision-tree algorithm is a supervised learning method based on a tree structure suitable for classification and regression tasks. By selecting and dividing the input features, the decision tree[36] builds a model that can match the appropriate motion-control and trajectory-planning strategies according to the different reagent characteristics.

The first step involved in algorithm implementation was determining the density, viscosity, and surface tension of each reagent, along with their corresponding recommended motion-control parameters. An appropriate model selected from the decision-tree classification, decision-tree regression, and random-forest models was chosen for each nonlinear output parameter based on the requirements and desired outcomes. During model training, the feature data (X) and corresponding results (Y) from the training set were transformed for optimal processing. Once the model achieved accurate predictions, it was saved for further application (Fig. S6A, S6B).

After training the models for all output parameters, the density, viscosity, and surface tension data of a new reagent were input. These data were fed into each corresponding model to generate predictive results. These results were then organised into an array, yielding a tailored motion-control and trajectory-planning strategy corresponding to the characteristics of the reagent (Fig. S6C,S6D).Decision Tree Operation Steps as follows:

♢ Prepare multiple acquisition card files in the standardized format, each containing the selected options from the experiment and the parameter results of the corresponding generated script.

♢ Parse these standardized files using pre-written code to generate structured feature data.

♢ Split the data randomly into two subsets (4: 1 ratio), with the larger subset as the training set, the smaller as the test set, and optionally select a portion for the cross-validation set.

♢ Train and validate models using sklearn's DecisionTreeClassifier and LinearRegression for nonlinear and linear features, respectively, and save the trained models.

♢ Invoke the parsing interface after model training to analyze new acquisition card options and generate the required parameter scripts.

H. G'-Code Script and Macro-Definition Packaging for ADP operation

NEC_ADP utilises a G'-code programming approach, modelled after computer-numerical-control systems, to encapsulate control commands specifically tailored for pipetting functions, as follows:

♢ G108 L1 L2 L3 L4Definition: Load tips on channels 1, 2, 3, and 4. (Convention: L for Load, with 1-8 representing eight channels).

♢ G108 U1 U2 U3 U4Definition: Unload tips on channels 1, 2, 3, and 4. (Convention: U for Unload, with 1-8 representing eight channels).

♢ G109 A1E10F10 A2E20 F8 A3E30 F15 A4E40 F5Definition: ADP Channel 1 moves to an absolute coordinate of 10 μL at 10 mm/s; Channel 2 to 20 μL at 8 mm/s; Channel 3 to 30 μL at 15 mm/s; Channel 4 to 40 μL at 5 mm/s.

If the end coordinates and speeds are the same across the ADP pipetting channels, they can be combined as follows:

♢ G109 A1 A2 A3 A4E300 F20Definition: Channels 1-4 move to an absolute coordinate of 300 μL at a speed of 20 mm/s.

To enhance G'-Code script adaptability and enable intelligent matching with the motion-control parameters generated by the decision-tree algorithm, macro definitions were embedded within the G'-Code to call ADP motor trajectory-planning parameters - to execute specific functions, such as leading air gap, aspirate, trailing air gap, dispense speeds (V_m), acceleration (A_{mp}), deceleration (A_{mm}), and the volumes for leading and trailing airgaps (Fig. S6E).

Examples of simple macro-definition follow:

// Leading air gap on Channel 1 with LAGS1 speed

G117 A1 E#LAGV1# F#LAGS1#

// Channel 1 aspirates the ASPV1 liquid at the ASPS1 speed

G117 A1 E$#LAGV1#+#ASPV1#$ F#ASPS1#

// Trailing air gap in Channel 1 with TAGS1 speed

G117 A1 E $#LAGV1# + #ASPV1# + #TAGV1# $ F#TAGS1#

The operation process of the equipment is shown in Fig. 2.

I. NEC_ADP System Integration

We designed a standardised control interface at the device level to facilitate seamless communication between the pipettors and the various types of equipment. By modularising the pipettor system and utilising the OPC UA protocol, we abstracted a universal information model that enables smooth integration with critical devices such as LIMS and liquid handling workstations, simplifies the interactions between systems and enhances both flexibility and scalability.

In response to diverse market demands with respect to pipetting, our control system incorporates a standardised interface concept to include different manufacturers and throughput types. We developed a generalised pipettor model that captures the essential characteristics and core functions and maintains broad compatibility with different pipettor manufacturers and versions. This design anticipates future functional expansion and new hardware integration, laying a solid foundation for long-term system development and iterations.

The pipetting operations were classified into four categories (aspiration, dispensing, aliquoting, and blowout mixing) and precise volume control for each

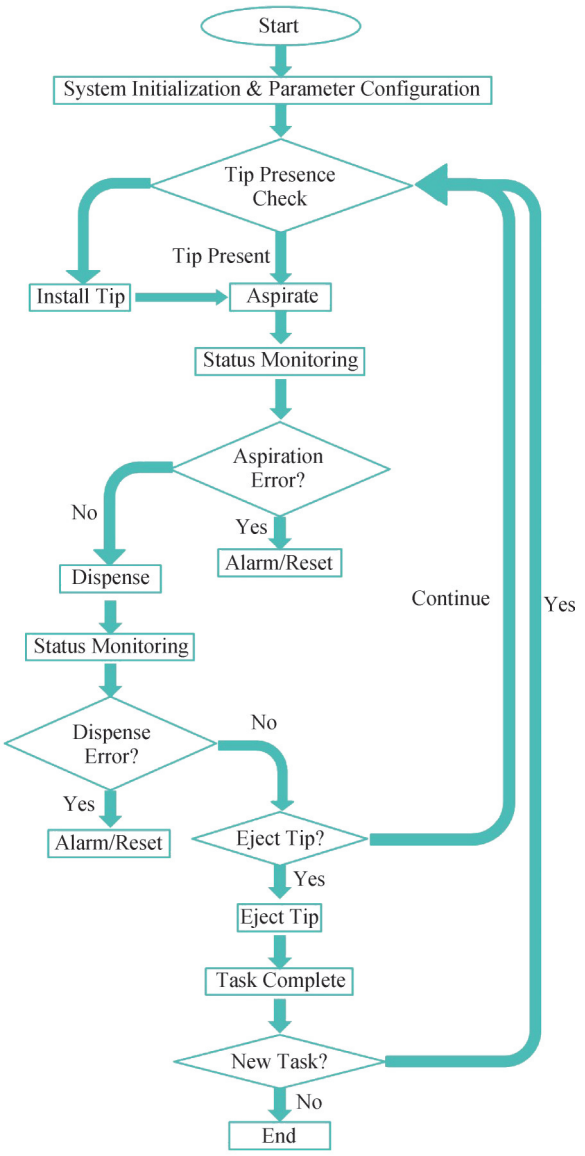

Fig.2 The workflow of the equipment operation.

category was implemented at various levels. We created a detailed controller-information model using the OPC UA protocol; this model covered the standard control interfaces for different experimental processes.

The NEC_ADP integration of a single-channel pipettor (NEC_ADP1_1) is illustrated in Fig. S7. The OPC UA (Fig. S7A) integrates both client and server modules with an innovative upper-layer application that serves client functions, providing intuitive data-node browsing and efficient data retrieval. Using the publish/subscribe mechanism of the OPC UA session, this system ensures real-time data-processing accuracy - thereby enhancing the responsiveness and reliability. We used the OPC UA modelling platform to construct a standardised information model for the basic pipettor types (Fig. S7B) and defined core attributes such as position, speed, and acceleration, while providing methods for configuring pipetting operations.

An important feature is that this model supports flexible expansion, allowing different manufacturers to build custom developments on a shared foundation and facilitating the seamless integration of various pipettor models and versions. The detailed sequence diagram (Fig. S7C) illustrates the execution of a single pipetting operation within the communication system; the efficient flow of command words between the client and server is highlighted; real-time feedback and operational efficiency are enhanced through query operation supplementation. This ensures high precision and efficiency in pipetting tasks.

The following equipment and materials were used for the NEC_ADP accuracy measurements and calibration experiments (Table S12).

♢ Guangzhou Chuangbo Plastic Mold Co., Ltd.: Liquid Reservoir CP01-WWYC, Tip Box CP01-TIP.

♢ Tecan (Shanghai) Laboratory Instruments Co., Ltd.: 1000 µL Pipette Tips 30000631, 50 µL Pipette Tips 30032114.

♢ Nanjing Duoli Yang Biotechnology Co., Ltd.: Lysis Plate DLY-24-FSP-150-F-S.

♢ Zhejiang Aijins Biotechnology Co., Ltd.: 96 Deep-Well Plate P-2.2-SQVT-96-P-S, Shallow-Well Plate P-0.5m l-SQV-96-S.

For further details, refer to Table S12.

3 Results

3.1 Application of NEC_ADP_1 in Automated Cell Culture

Cell-culture workflow involves transferring minimal (<5 µL) and large liquid volumes (>900 µL) -for tasks such as adding or preparing signalling-pathway-activator or -inhibitor reagents (such as growth factor/ROCK inhibitor)-or for performing media changes in multi-well plates (essential to ensure consistent nutrient delivery and reagent concentration). Systems are also required to incorporate features such as adjustable and adaptive dispense rates or specific pipetting algorithms (reverse pipetting) -to protect sensitive cell types and avoid damaging cells through excessive shear forces. Reagents in cell-culture workflows have varying densities, viscosities, and surface tensions (e. g. viscous solutions such as glycerol or volatile liquids such as ethanol). Automated systems must handle these liquids accurately without introducing errors in the volume transfer.

The NEC_ADP is a series of pipettes, available in one to eight channel configurations (NEC_ADP1_1 to NEC_ADP1_8). They operate individually, are compatible with various standard plate formats, and offer significant advantages for high-precision biological experiments. These pipettes are suitable for cell-culture-related tasks and other biological processes that require precise fluid control, even when the throughput demands are not exceptionally high. For instance, they were integrated into our self-developed, fully automated stem-cell induction and culture platform (Fig. 3A) [33]; this platform combines functions such as cell culture,

(A)

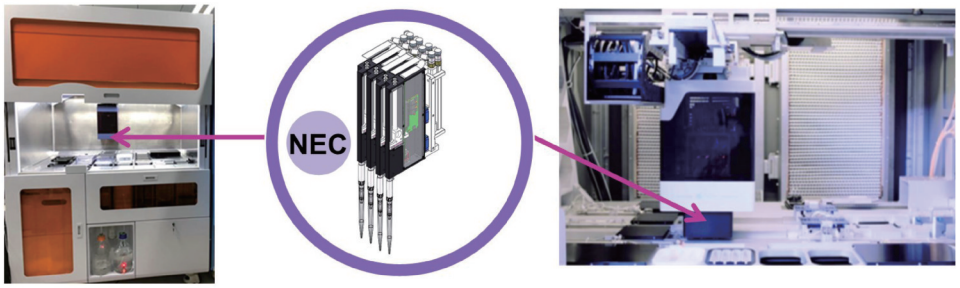

(B)

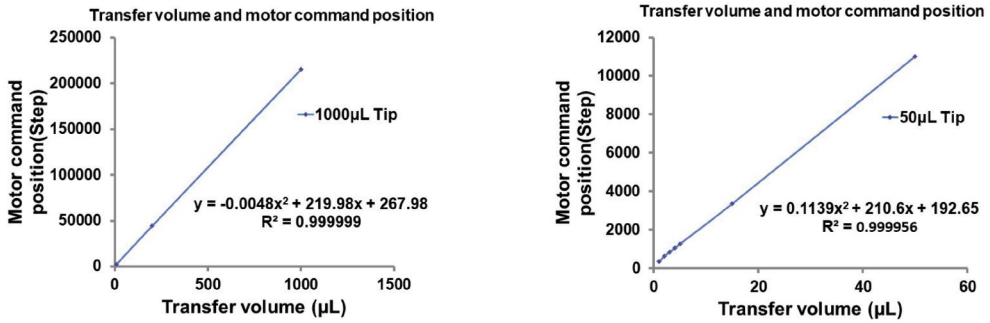

(C)

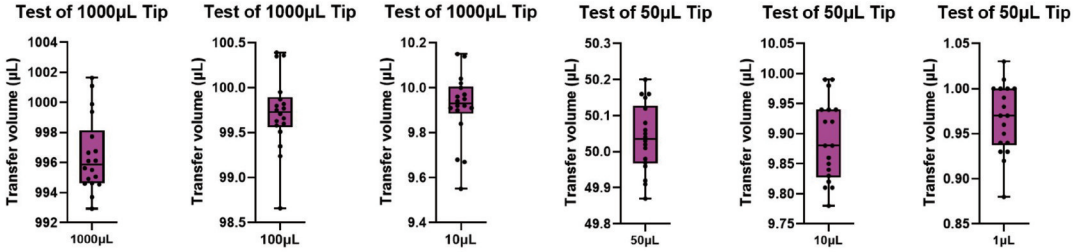

(D)

Tip	1000μL						50μL							
Volume	1000μL		100μL		10μL		50μL		10μL		5μL		1μL	
ADP	TECAN Cavro®	NEC_ADP 1_4	TECAN Cavro®	NEC_ADP 1_4	TECAN Cavro®	NEC_ADP 1_4	TECAN Cavro®	NEC_ADP 1_4	TECAN Cavro®	NEC_ADP 1_4	TECAN Cavro®	NEC_ADP 1_4	TECAN Cavro®	NEC_ADP 1_4
Inaccuracy (Systematic error)	1.0%	0.35%	2.0%	0.28%	7.5%	0.85%	2.0%	0.07%	3.0%	0.68%	5.0%	0.98%	5.0%	3.30%
Imprecision （Random error）	0.75%	0.25%	0.75%	0.41%	3.5%	1.56%	0.75%	0.19%	1.0%	1.09%	2.0%	1.33%	6.0%	3.98%

(E)

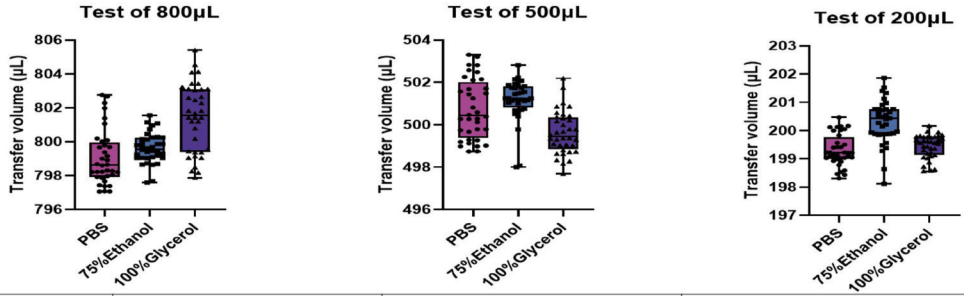

(F)

Volume	800μL			500μL			200μL		
Reagent	PBS	75% Ethanol	100% Glycerol	PBS	75% Ethanol	100% Glycerol	PBS	75% Ethanol	100% Glycerol
Max Inaccuracy (Systematic error)	0.25%	0.10%	0.41%	0.48%	0.31%	0.27%	0.45%	0.32%	0.39%
Max Imprecision （Random error）	0.26%	0.16%	0.26%	0.27%	0.35%	0.24%	0.42%	0.48%	0.26%

Fig.3 NEC_ADP_1 performance in accuracy with various reagents. (A) NEC_ADP_1 series expanded to a four-channel configuration, NEC_ADP1_4, enabling its application in fully automated stem-cell induction and large-scale mesenchymal stem-cell production. It primarily handles the transfer of 1000 μL volumes of culture medium, ethanol, and PBS, as well as precise transfers of small volumes ranging from 50-1 μL. (B) Resolution (Resolution_SV) of the NEC_ADP_1 was tested using gravimetric methods with 1000 and 50 μL pipette tips; this resulted in a regression curve showing the relationship between pipetted volume and motor-command position. (C) Test of NEC_ADP_1 for the 1000 and 50 μL tips. (D) Comparison of inaccuracy and imprecision between the NEC_ADP_1 and the TECAN Cavro® pipette (Table S7). (E) Using a 1000 μL pipette tip, volumes of 800, 500, and 200 μL of reagents of varying density, viscosity, and surface tension (e.g., PBS, 75% ethanol, and 100% glycerol) were transferred to measure inaccuracy and imprecision, and a database was established (Table S2). (F) Full-stroke errors for inaccuracy and imprecision while handling PBS, 75% ethanol, and 100% glycerol were all below 0.5% (Table S3, Table S4, Table S5). Eighteen measurements were conducted in this study.

monitoring, liquid handling, and algorithm-based identification, and it enables automated induction and culture of induced pluripotent stem cells, mesenchymal stem cells, and organoid formation.

NEC technology was applied to the NEC_ADP1_1 model, where gravimetric testing was used to assess the resolution (Resolution_SV) of pipetting with both 1000 and 50 μL tips (Fig. 3C, Table S6), generating a regression curve of pipetting volume versus motor-command position (Fig. 3B).

3.1.1 Regression Equation for 1000-μL Pipette Tip

$$y = -0.0048x^2 + 219.98x + 267.98 \quad (R^2 = 0.999999)$$

3.1.2 Regression Equation for 50-μL Pipette Tip

$$y = 0.1139x^2 + 210.6x + 192.65 \quad (R^2 = 0.999956)$$

where x is the target volume and y is the motor-command position.

The test results indicated that both the inaccuracy and imprecision of NEC_ADP1_1 were within 5%, outperforming those of the TECAN pipette (Fig. 3D, Fig. S3). NEC_ADP1_1 also demonstrated excellent performance across various specialised reagents, with a full-stroke error below 0.5%, and was suitable for ethanol, glycerol, PBS, and other reagents (Fig. 3E, Fig. 3F, Fig. S2, Table S3-S5), thereby providing robust support for high-precision biological experiments. Expanding NEC_ADP1 to a four-channel configuration (NEC_ADP1_4) met the diverse pipetting requirements of stem-cell culture (Table S7, Fig. S3), validating its applicability and supporting fully automated stem-cell induction and large-scale mesenchymal stem cell production [33].

Based on the precision test data for the NEC_ADP_1 series, these pipettes achieve exceptional performance in transferring volumes of 1000, 50, and even 1 μL through NEC technology. Tests with multiple specialised reagents demonstrated full-stroke error rates below 0.5%, surpassing the performance of Tecan Cavro® pipettes. Furthermore, the NEC_ADP_1 series supports configurations from one to eight channels, accommodating diverse, independent or synchronised, pipetting tasks in automated stem-cell induction and the preparation of other differentiated cell types, thereby providing strong support for high-precision biological experimentation.

3.2 Application of NEC_ADP_4 in Trace Nucleic-Acid Extraction and Synthetic-Biology Automation

Automated liquid-handling systems are indispensable for trace nucleic-acid extraction and synthetic biology automation because they provide the precision, consistency, and scalability needed to handle ultralow volumes, while minimising errors and contamination risks[34]. Trace nucleic-acid extraction and synthetic-biology workflows frequently involve transferring micro-volumes (1-10 μL), of reagents like polymerase chain reaction (PCR) mixes, primers, or enzymes. Moreover, the reagents used in these workflows, such as ethanol or buffer solutions, have diverse properties, such as varying viscosity, surface tension, and volatility. Precise volume handling requires the system to adapt pipetting speeds and control techniques for these liquid characteristics to ensure accurate dispensing.

The four-channel inline pipette system NEC_ADP_4 (Fig. S4C) is a key component in high-throughput, high-sensitivity nucleic acid diagnostic automation, and plays a critical role in ultra-micro-DNA extraction systems. This method is widely applicable to nucleic-acid extraction from various trace samples. Additionally, this module was utilised within synthetic biology platforms (Fig. 4A) to enable automated extraction, preparation, and detection of bacterial DNA, particularly from *E. coli*.

The core of the ultra-micro-DNA extraction system and synthetic-biology platform was a robotic liquid-handling module composed of two NEC_ADP_4 units forming an eight-channel pipette (NEC_ADP4_8). This module ensures efficient and precise liquid handling through precise control and accommodates diverse experimental requirements. For specific pipetting volumes, we tested Resolution_SV of 1000, 50, and 10 μL pipette tips when transferring various liquid volumes (Table S8, Figs. 3B, 3D, 3F), constructing NEC regression curves (Figs. 3C, 3E, 3G):

3.2.1 Regression Equation for 1000-μL Pipette Tip

$$y = -0.0011x^2 + 213.35x + 230.5 \quad (R^2 = 0.999999)$$

3.2.2 Regression Equation for 50-μL Pipette Tip

$$y = 0.0554x^2 + 211.37x + 153.96 \quad (R^2 = 0.999996)$$

3.2.3 Regression Equation for 10-μL Pipette Tip

$$y = 0.6467x^2 + 204.64x + 126.25 \quad (R^2 = 0.999827)$$

where x is the target volume and y is the motor-command position.

The Eppendorf epMotion® automated liquid-handling systems offer mechanically shifting a range of modulated dispensing tools to accommodate various volume requirements. Examples of different modules with different operating ranges and accuracies follow: TM 10-8: 0.2-10 μL (8-channel); TM 50-8: 1-50 μL (8-channel); TM 300-8: 20-300 μL (8-channel); and TM 1000-8: 40-1, 000 μL (8-channel) (Table S9B). Comparative analysis indicates that the one-module full range NEC_ADP4_8, equipped with an NEC algorithm, demonstrates advantages over the Eppendorf epMotion® series eight-channel dispensing tools (TM 1000-8 and TM 50-8) in terms of pipetting accuracy and precision (Fig. 4H, Fig. 4I). NEC_ADP4_8 performs exceptionally within the 5-1000 μL volume range, significantly

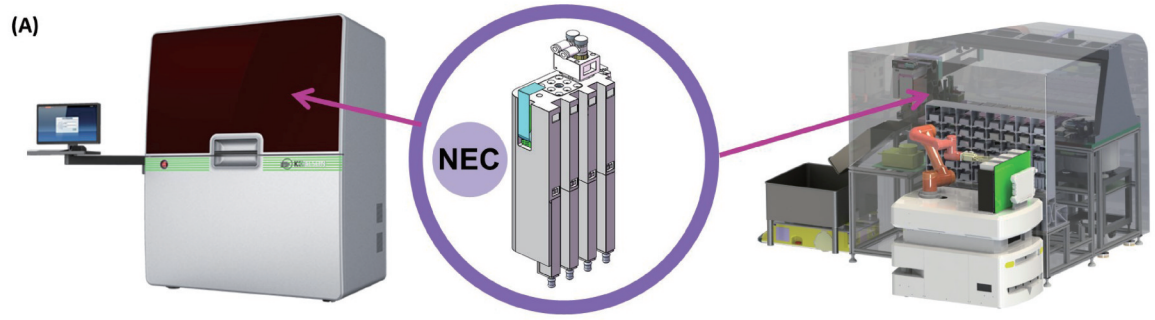

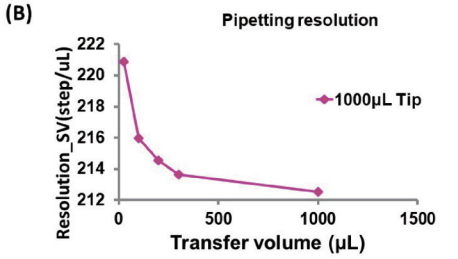

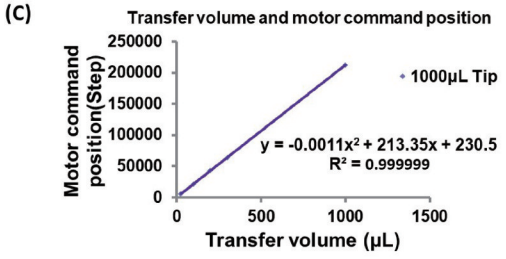

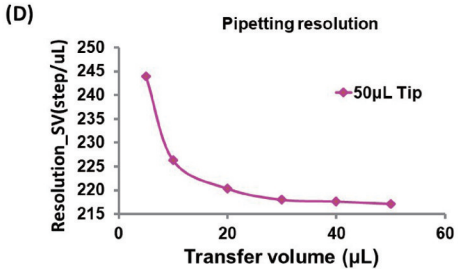

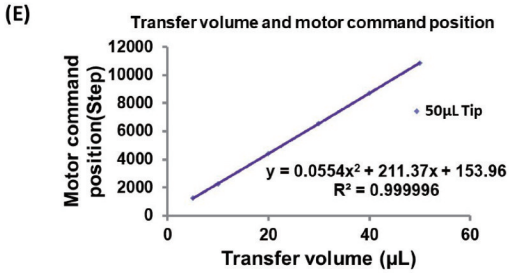

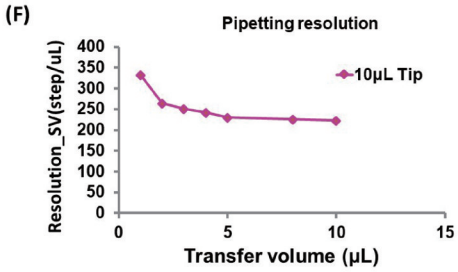

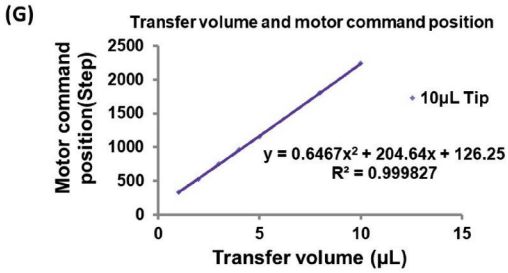

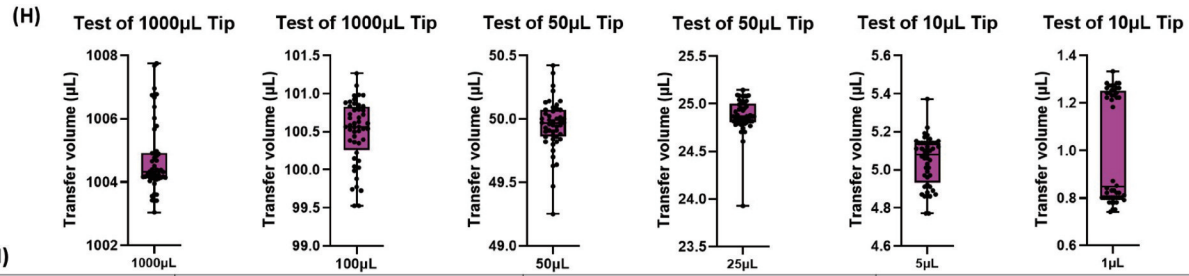

(I)

Tip	1000μL				50μL				10μL			
Volume	1000μL		100μL		50μL		25μL		5μL		1μL	
ADP	TM 1000-8	NEC_ADP4_8	TM 1000-8	NEC_ADP4_8	TM 50-8	NEC_ADP4_8	TM 50-8	NEC_ADP4_8	TM 50-8	NEC_ADP4_8	TM 50-8	NEC_ADP4_8
Inaccuracy (Systematic error)	0.8%	0.47%	3.0%	0.5%	1.2%	0.1%	2.0%	0.49%	5%	0.92%	25.0%	0.91%
Imprecision （Random error）	0.15 %	0.11%	1.5%	0.41%	0.6%	0.41%	1.2%	0.75%	5%	2.54%	10.0%	22.61%

Fig.4 Accuracy of the Eight-Channel NEC_ADP4_8. (A) Four-channel inline pipette NEC_ADP_4 applied in ultra-micro-DNA extraction equipment and synthetic-biology automation platforms. (B) Resolution_SV when pipetting with a 1000 μL tip. (C) Regression curve of pipetted volume versus motor-command position for the 1000 μL tip. (D) Resolution_SV when pipetting with a 50 μL tip. (E) Regression curve of pipetted volume versus motor-command position for the 50 μL tip. (F) Resolution_SV when pipetting with a 10 μL tip. (G) Regression curve of pipetted volume versus motor-command position for the 10 μL tip. (H) Test of NEC_ADP4_8 for the 1000, 50, and 10 μL tips. (I) Comparison of inaccuracy and imprecision between NEC_ADP4_8 and the Eppendorf 8-channel pipette (Table S9). Forty-eight measurements were conducted in this study.

reducing inaccuracy and imprecision (Table S9A). However, for pipetting volumes between 1 and 5 μL, the NEC_ADP4_8 with a 1000- μL volume-range is less accurate than the Eppendorf epMotion® with a 10- μL volume-range pipette (TM 10-8)[30-33].

In this study, a comparative analysis was conducted to evaluate the pipetting accuracy and precision of NEC_ADP4_8 using an NEC algorithm. Results showed that the NEC_ADP4_8 significantly improves accuracy over the Eppendorf epMotion® series eight-channel dispensing tools (TM 1000-8 and TM 50-8), particularly in the 5-1000 μL range. The application of NEC technology enhanced the pipetting precision of NEC_ADP4_8, allowing high-accuracy pipetting over a broad volume range without hardware adjustments.

3.3 Application of NEC_ADP_96 in Scaled Drug Screening and High-Throughput Sequencing Library Preparation

Ensuring uniform volume delivery across multiple channels (e. g. 96 or 384 well plates) is critical in high-throughput setups. Automation ensures channel-to-channel consistency and eliminates variability that can compromise experimental results. Many protocols require transferring ultra-low volumes (for instance, around 1 μL) of reagents, especially in nucleic acid workflows like library preparation or qPCR setup. Achieving precision on this scale requires highly accurate pipetting mechanisms and robust calibration designs.

The 96-channel integrated pipette system NEC_ ADP_96 (Fig. S4D) served as a core module for high-depth library construction, which is essential for tasks such as drug-compound library screening, organoid-cell selection, and single-cell next-generation library preparation (Fig. 5A). This system is crucial for high-throughput workflows that require consistent small-volume automation. In single-cell high-throughput library construction, NEC_ADP96 integrates key processes, including sample reception, PCR, complex pipetting sequences, washing, and fluorescent dispensing, enabling efficient automation. With its robotic arm-driven liquid-handling module and 96-channel parallel pipetting capability, NEC_ADP_96 dramatically enhances the operational efficiency and precision.

For trace liquid-transfer needs in library preparation - such as handling RT-mix, PreAmp-mix, XP-beads, ethanol, ddH2O, Tagm-mix, Enrchm-mix+index, XP-beads, and standard DNA - pipetting tasks are concentrated on volumes below 50 μL. The 50 μL pipette tip on the NEC_ADP_96 effectively manages these requirements, ensuring high precision even for minimal liquid transfers. The resolution of the 50 μL tip across various liquid volumes was tested and summarised in Table S10 and Fig. 5B, and a regression curve of pipetted volume versus motor command was constructed (Fig. 5C):

3.3.1 Regression Equation for 50-μL Pipette Tip

$$y = -1.2271x^2 + 1514x + 624.04 \quad (R^2 = 0.999997)$$

where x is the target volume and y is the motor-command position.

Based on the regression curve, an NEC strategy was introduced and compared with the Hamilton CO-RE 96-channel pipette (Table S11). Results indicate that the NEC_ADP_96 demonstrated superior accuracy and precision to the Hamilton CO-RE 96 when pipetting 1, 5, and 50 μL volumes (Fig. 5D, Fig. 5E).

3.3.2 NEC Algorithm Application in Commercial Hardware (Tecan Cavro) as a Generalised Method

The NEC technique significantly enhances the performance of commercial pipetting systems. For instance, a Tecan Cavro® pipette (S/N: 1701000076, P/N: 30041734) was evaluated as a case study (Fig. 6A). Using gravimetric analysis, the accuracy of the Tecan Cavro® pipette equipped with a 1000-μL pipette tip was tested for liquid volumes of 1000, 100, and 10 μL (Fig. 6B). The results indicated a substantial decline in accuracy compared to the factory-calibrated precision reported in previous testing[29], with the inaccuracy being particularly pronounced.

To address this, a regression formula was adapted to optimise the command positions based on actual data obtained through gravimetric analysis rather than relying on Resolution_SV for nonlinear compensation. This resulted in a newly constructed regression curve describing the relationship between target and command volumes (Fig. 6A).

3.3.3 Regression Equation for the 1000 μL Pipette Tip

$$y = 0.000001x^2 + 1.0096x + 1.1961 \quad (R^2 = 0.999999)$$

where x represents the target volume and y represents the command volume.

For example, when the target volume x is 10 μL, the corrected command volume y, calculated using the regression equation, is 11.292 μL, corresponding to the command: "/1A11.292,1R." Similarly, for a target volume of 100 μL, the compensated command volume is 102.166 μL, corresponding to the command: "/1A102.166,1R."

Testing results revealed that applying NEC significantly improved the Tecan Cavro® pipette performance. The inaccuracies and imprecisions for transferring volumes of 1000, 100, and 10 μL were effectively controlled to within 6%, with a notable improvement in accuracy (Fig. 6B, Fig. 6C).

In summary, the NEC technique enables on-site calibration of the Tecan Cavro pipette, eliminating the need for factory recalibration. Pipetting precision was significantly improved by recalibrating the system with NEC. This demonstrated that NEC is not limited only to in-house custom-developed ADP systems but can be applied to commercial hardware, showing broad generalisability and potential for widespread implementation.

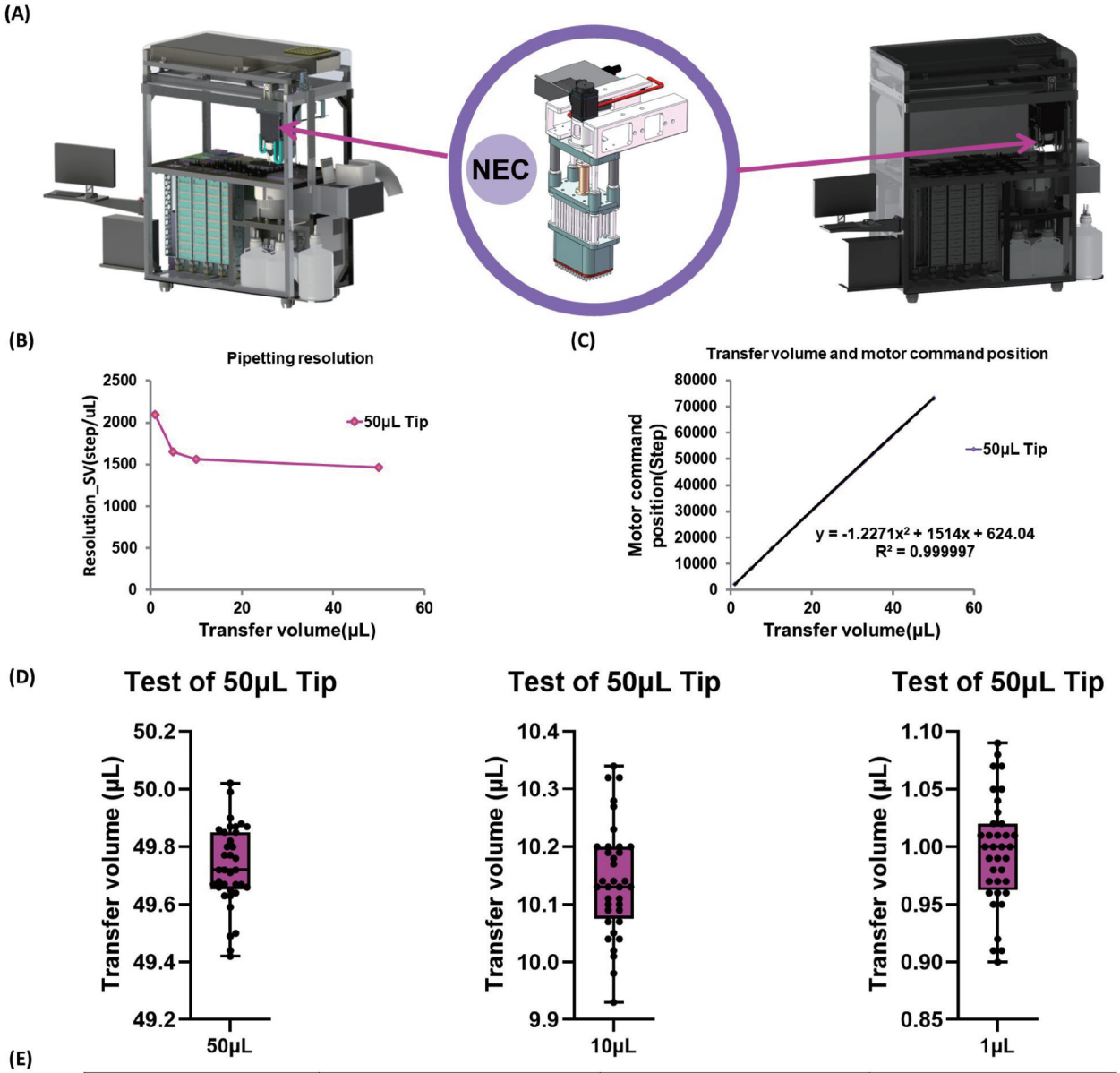

(E)

Volume	50μL		10μL		1μL	
ADP	Hamilton CO-RE 96*[4]*	NECADP96	Hamilton CO-RE 96*[4]*	NECADP96	Hamilton CO-RE 96*[4]*	NECADP96
Inaccuracy (Systematic error)	1.5%	0.54%	2.5%	1.75%	5%	0.44%
Imprecision（Random error）	1.0%	0.28%	2%	1.08%	5%	4.76%

Fig.5 Accuracy of the 96-Channel Integrated Pipette NEC_ADP_96. (A) 96-channel integrated pipette NEC_ADP_96 applied in high-depth library-construction equipment. (B) Resolution for pipetting with the 50 μL tip. (C) Regression curve of pipetted volume versus motor-command position for the 50 μL tip on the 96-channel pipette. (D) Test of NEC_ADP96 50, 10, and 1 μL for the 50 μL tip. (E) Comparison of inaccuracy and imprecision for the 50 μL tip (Table S11). Thirty-six measurements were conducted in this study.

4 Discussion

This study introduces a novel NEC model that integrates trajectory planning optimization with motor control automation for pipetting systems. The NEC framework dynamically correlates motor displacement deviations to pipetting errors through a decision tree-driven parameter selection mechanism, overcoming the limitations of conventional linear calibration methods while ensuring adaptive strategy matching. The method was successfully implemented in the NEC_ADP series pipettes, including single-channel NEC_ADP_1, inline multichannel NEC_ADP_4, and integrated 96-channel NEC_ADP_96, enabling seamless scalability from single-channel to multichannel configurations.

The NEC_ADP series of pipettes exhibited exceptional performance in practical applications. In high-precision biological experiments, high-throughput, high-sensitivity nucleic-acid diagnostic systems, and high-

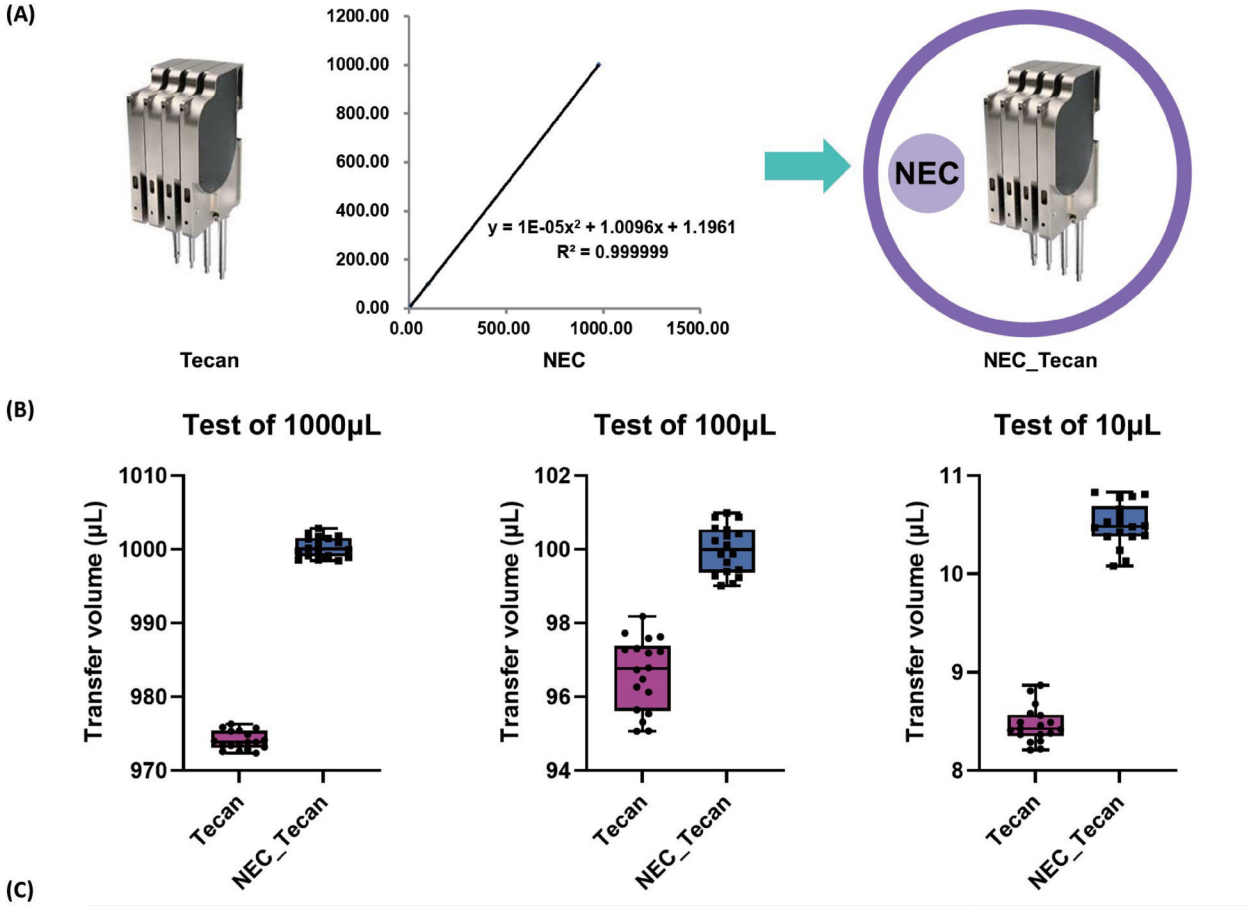

(C)

Volume	1000μL		100μL		10μL	
ADP	Tecan	NEC_Tecan	Tecan	NEC_Tecan	Tecan	NEC_Tecan
Max Inaccuracy (Systematic error)	2.62%	0.12%	3.52%	0.71%	15.73%	5.60%
Max Imprecision （Random error）	0.17%	0.16%	1.42%	0.59%	2.88%	3.06%

Fig.6 Application of Nonlinear Error Compensation Technology to Commercial Pipettes. (A) NEC technique application to a commercial Tecan Cavro® pipette (NEC_Tecan). A new regression curve was constructed by adjusting the regression formula and optimising command positions based on experimental data. (B) Comparative test using a 1000-μL pipette tip to evaluate the pipetting performance of the standard Tecan Cavro® and the NEC_Tecan system. (C) Comparison of inaccuracy and imprecision between the standard Tecan Cavro® pipette and the NEC_Tecan system demonstrating improved performance achieved by applying NEC technology. Eighteen measurements were conducted in this study.

depth library construction, the NEC_ADP series consistently delivered stable and precise liquid-handling solutions. Its online, precision-calibration functionality ensured real-time error detection and correction and maintained long-term pipetting accuracy. In addition, a specialised database was developed for pipetting experiments involving reagents with diverse properties. By leveraging decision-tree algorithms from machine learning, the system achieved intelligent matching of motion control and trajectory-planning strategies, ensuring precise pipetting for all reagent types. Although the NEC_ADP4_8 pipette demonstrated remarkable pipetting precision and broad volume range coverage across various research and industrial applications, its performance in the micro-volume range of 1-5 μL was slightly inferior to that of the Eppendorf epMotion® series 10-μL pipette (TM 10-8)[14-20]. This indicates that the mechanical design of NEC_ADP_4, whose tip geometry and fluidic resistance are precision-engineered to match low-volume dynamics, could benefit from further optimisation to enhance its performance within this specific volume range.

Integrating decision-tree algorithms from machine learning to achieve intelligent methods with online calibration technology enables the precise handling of diverse liquids in various pipetting scenarios. This integrated approach allowed NEC_ADP to enhance the pipetting accuracy through nonlinear compensation and precise trajectory planning, and online precision calibration ensured that the pipetting accuracy could meet the required standards. The application of NEC technology to the Tecan Cavro® pipette also significantly improved performance across various liquid volumes. Thus, this technology is not only suitable for custom-

developed ADP systems, but also applicable to other commercial devices. The system supports on-site recalibration, eliminating the need for factory calibration. This underscores the versatility and potential for its widespread adoption.

The Tecan Cavro® ADP was selected as a representative commercial system, as it is the most representative product in the industry [35], to rigorously validate the core principles of our nonlinear error compensation framework. While the current study focuses on demonstrating NEC's efficacy in this widely adopted platform, the methodology itself is mechanically agnostic—its software-driven calibration and adaptive algorithms target universal sources of volumetric error (e. g., stepper motor nonlinearity, plunger hysteresis), rather than specific hardware configurations. For other brands, minor parameter adjustments (e. g., motor step-response coefficients) may be required, but the core compensation logic remains applicable.

In future work, we aim to reduce operational inaccuracies by optimising mechanical processing and assembly precision, thereby providing users with more reliable and efficient experimental solutions. Artificial intelligence will be employed to achieve closed-loop adjustments of the NEC_ADP nonlinear error model, further enhancing the pipetting accuracy and system performance. We plan to collect extensive operational data from NEC_ADP and perform data pre-processing and feature extraction. We trained an error-prediction model using machine learning or deep-learning algorithms and refined the model based on evaluation outcomes. We plan to explore different model algorithms, adjust the model parameters, and use feature-selection methods to establish a more robust NEC model. This trained error-prediction model will then be integrated into the automated pipetting system, enabling real-time prediction of the NEC_ADP nonlinear compensation coefficient, along with continual optimisation of the prediction model and closed-loop control algorithm, to further improve the pipetting accuracy and system performance.

5 Conclusion

In conclusion, the NEC_ADP series of pipettes, with their modular packaging and operation on an open platform communications unified architecture bus, enable seamless integration with diverse automated equipment and LIMS systems. This design enhances the rapid integration capability, allowing for flexible applications across various life-science instruments and swift deployment in laboratory environments. Incorporating NEC technology significantly improves pipetting efficiency and accuracy, making NEC_ADP a vital tool for advanced applications in the life sciences. These methods include stem-cell preparation, high-throughput diagnostic analyses, synthetic biology, and genomic library construction. By addressing the critical needs for precision and scalability, the NEC_ADP series and its NEC technology strongly support rapid advancements in life-science research and innovation.

Author Contribution:

J. L. and Z. Z. contributed equally to this work. Conceptualization: J. L., X. Z, G. Z., and X. C., Methodology: J.L., G. Z., X.C., Z.Z., Q.Y.,Y.W., J.Q., and G.S., Investigation: J.L., Z.Z., X.C., Q.Y., S.Z., Y.W., J. C., G.S., Z.S., J.D., J.Q., and S.M., Funding acquisition: J. L., X.Z, and X.C., Project administration: J.L., F.Z., and X. W., Supervision: G. Z. and X. Z., Writing—original draft: J.L., Q.Y., and Z.Z., Writing—review and editing: J. L., X.Z., G.Z., and X.C.

Funding Information:

This study was supported in part by the National Key R&D Program of China [Grant No. 2023YFF0724200], Strategic Priority Research Program of the Chinese Academy of Sciences [Grant No. XDB1250000], Key Research and Development Program of Guangzhou City [Grant No. 2024B03J0002, 2025B03J0095], and in part by the Guangzhou Koalson Smart Manufacturing Technology Co., Ltd., Scientific Instrumentation Development Program of Chinese Academy of Sciences [Grant No. PTYQ2024TD0002, ZDKYYQ20210006], Key Research Program of Chinese Academy of Sciences [Grant No. ZDBS-ZRKJZ-TLC006], Guangzhou Basic and Applied Basic Research Project [Grant No. 2024A04J6352, 2022A1515110435], Human Cell Lineage Atlas Facility [Grant No. DSS05010101], Basic Research Project of Guangzhou Institutes of Biomedicine and Health, Chinese Academy of Sciences [No. GIBHBRP24-03].

Conflicts of Interest:

The authors declare that they have no competing interests.

Data Availability Statement

All data needed to evaluate the findings are present in the paper and/or the Supplementary Material.

Dates:

Received 18 August 2025; Accepted 17 March 2026; Published 31 March 2026

Supplementary Material:

The Supplementary Material file includes:

1. Figs. S1 to S8

2. Tables S1 to S12

References

[1] Carasek E, Morés L, Huelsmann RD. Disposable pipette

extraction: A critical review of concepts, applications, and directions. Analytica Chimica Acta, vol. 1192, no. 3, pp. 339383, **2022**.

[2] Guan XL, Chang DPS, Mok ZX, et al. Assessing variations in manual pipetting: An under-investigated requirement of good laboratory practice. Journal of Mass Spectrometry and Advances in the Clinical Lab, vol. 30, no. 1, pp. 25-29, **2023**.

[3] Lin TJ, Beal KM, Brown PW, et al. Evolution of a comprehensive, orthogonal approach to sequence variant analysis for biotherapeutics. MAbs, vol. 11, no. 1, pp. 1-12, **2019**.

[4] Https://www. Hamiltoncompany. Com/oem/oem-components/pipette-channels#resources. Aug. 30, 2025:

[5] Gregor BW, Coston ME, Adams EM, et al. Automated human induced pluripotent stem cell culture and sample preparation for 3d live-cell microscopy. Nature Protocols, vol. 19, no. 2, pp. 565-594, **2024**.

[6] Viana MP, Chen J, Knijnenburg TA, et al. Integrated intracellular organization and its variations in human ips cells. Nature, vol. 613, no. 7943, pp. 345-354, **2023**.

[7] Bush EC, Ray F, Alvarez MJ, et al. Plate-seq for genome-wide regulatory network analysis of high-throughput screens. Nature Communications, vol. 8, no. 1, pp. 105, **2017**.

[8] Https://partnering. Tecan. Com/cavro-air-displacement-pipettor-for-oem-liquid-handling. Aug. 30, 2025:

[9] Liu H, Zeng Q, Zhou J, et al. Single-cell DNA methylome and 3d multi-omic atlas of the adult mouse brain. Nature, vol. 624, no. 7991, pp. 366-377, **2023**.

[10] Barak N, Ben-Ami R, Sido T, et al. Lessons from applied large-scale pooling of 133, 816 sars-cov-2 rt-pcr tests. Sci Transl Med, vol. 13, no. 589, pp. 1-7, **2021**.

[11] Smyrlaki I, Ekman M, Lentini A, et al. Massive and rapid covid-19 testing is feasible by extraction-free sars-cov-2 rt-pcr. Nature Communications, vol. 11, no. 1, pp. 4812, **2020**.

[12] Peng Q, Liu X, Li W, et al. Analysis of blood methylation quantitative trait loci in east asians reveals ancestry-specific impacts on complex traits. Nature Genetics, vol. 56, no. 5, pp. 846-860, **2024**.

[13] Safieddine A, Coleno E, Lionneton F, et al. Ht-smfish: A cost-effective and flexible workflow for high-throughput single-molecule rna imaging. Nature Protocols, vol. 18, no. 1, pp. 157-187, **2023**.

[14] Https://www.Eppendorf.Com/. Aug. 30, 2025:

[15] Song X, Zhang H, Zhang Y, et al. Gut microbial fatty acid isomerization modulates intraepithelial t cells. Nature, vol. 619, no. 7971, pp. 837-843, **2023**.

[16] Rosshart SP, Herz J, Vassallo BG, et al. Laboratory mice born to wild mice have natural microbiota and model human immune responses. Science, vol. 365, no. 6452, pp. 1-29, **2019**.

[17] Tm 1000-8 eight-channel dispensing tool. Https://www. Eppendorf. Com/dk-en/products/automated-pipetting/liquid-handler-accessories/epmotion-dispensing-tools-p-5280000258. Aug. 30 , 2025:

[18] Tm 50-8 eight-channel dispensing tool. Https://www. Eppendorf. Com/dk-en/products/automated-pipetting/liquid-handler-accessories/epmotion-dispensing-tools-p-5280000215. Aug. 30 , 2025:

[19] Tm 300-8 eight-channel dispensing tool. Https://www. Eppendorf. Com/dk-en/products/liquid-handling/automation-accessories/epmotion-dispensing-tools-p-5280000231. Aug. 30 , 2025:

[20] Tm 10-8 eight-channel dispensing tool. Https://www. Eppendorf. Com/dk-en/products/automated-pipetting/liquid-handler-accessories/epmotion-dispensing-tools-p-5280000304. Aug. 30 , 2025:

[21] Murakami H, Yamada N. Speed and accuracy tradeoff in whole body movement during vertical jumps under varying landing constraints. Scientific Reports, vol. 15, no. 1, pp. 19966, **2025**.

[22] Erwinski K, Wawrzak A, Paprocki M. Real-time jerk limited feedrate profiling and interpolation for linear motor multiaxis machines using nurbs toolpaths. IEEE Transactions on Industrial Informatics, vol. 18, no. 11, pp. 7560-7571, **2022**.

[23] Hamed KA, Kamidi VR, Ma WL, et al. Hierarchical and safe motion control for cooperative locomotion of robotic guide dogs and humans: A hybrid systems approach. IEEE Robotics and Automation Letters, vol. 5, no. 1, pp. 56-63, **2020**.

[24] Https://www.Iso.Org/obp/ui/en/#iso:Std:Iso:8655:-6:Ed-2:V2:En iso 8655-6:2022: The high art of pipette calibration. Aug. 30, 2025:

[25] Https://www. Integra-biosciences. Com/united-states/en/pipetting-tips-improve-accuracy-and-precision. Aug. 30, 2025:

[26] Mai C, Wang Z, Chen L, et al. Field-based calibration and operation of low-cost sensors for particulate matter by linear and nonlinear methods. Atmospheric Pollution Research, vol. 16, no. 12, pp. 102676, **2025**.

[27] Prasad PJ, Bodhe GL. Trends in laboratory information management system. *Chemometrics and Intelligent Laboratory Systems* , vol. 118, no. pp. 187-192, 2012.

[28] Johnson T. Integrating lims and chromatography data systems. Laboratory Automation & Information Management, vol. 34, no. 1, pp. 69-74, **1999**.

[29] Chen Y, Lin Y, Yuan X, et al. Lims and clinical data management. In: SHEN B, TANG H, JIANG X. *Translational biomedical informatics: A precision medicine perspective* . Singapore: Springer Singapore. 2016. 225-239

[30] Https://scikit-learn. Org/stable/modules/generated/sklearn.Tree.Decisiontreeclassifier.Html. Aug. 30, 2025:

[31] Lu J, Zhang Z, Zhang S, et al. A machine learning-driven robotic system for autonomous nucleic acid extraction and library preparation. *SLAS Technol* , vol. 35, no. pp. **100370**, 2025.

[32] Sorbello M, Micaglio M, Zdravkovic I, et al. Pressure, volume and temperature: Boyle's law rules airways. Minerva Anestesiol, vol. 84, no. 9, pp. 1112-1114, **2018**.

[33] Chen X, Fan K, Lu J, et al. Selecting monoclonal cell lineages from somatic reprogramming using robotic-based spatial-restricting structured flow. *Research* , vol. 7, no. pp. Article ID 0338, **2024**.

[34] Lu J, Fan W, Huang Z, et al. Automatic system for high-throughput and high-sensitivity diagnosis of sars-cov-2. Bioprocess Biosyst Eng, vol. 45, no. 3, pp. 503-514, **2022**.

[35] Https://www. Tecan. Com/hubfs/hubdb/te-docdb/pdf/br_cavro_air_displacement_pipettor_396359. Pdf. Aug. 30, 2025: